Processing and Application of Ceramics 13 [2] (2019) 132–138
https://doi.org/

Examination of novel electrosprayed biogenic hydroxyapatite coatings on Si_3N_4 and Si_3N_4/MWCNT ceramic composite

Tamás Zagyva, Katalin Balázsi, Csaba Balázsi*

Centre for Energy Research, Hungarian Academy of Sciences, Konkoly-Thege str. 29-33, 1121 Budapest, Hungary

Received 28 October 2018; Received in revised form 5 February 2019; Accepted 23 April 2019

Abstract

Novel hydroxyapatite coatings on Si_3N_4 and Si_3N_4/MWCNT ceramic substrates were deposited by electrospraying method for the first time. The aim of this study was to produce thin nano-hydroxyapatite (nHA) layer on silicon nitride (Si_3N_4) implant material with a cost-efficient electrospray deposition method. During the first experiments, continuous nHA layer could not form due to the high electrical resistance of the Si_3N_4 substrate. Therefore, the electrical conductivity of the Si_3N_4 substrate has been increased by the help of multiwall carbon nanotube (MWCNT) addition. As a result, ~5 μm thick continuous and smooth nHA coating could have been realized successfully on the Si_3N_4/MWCNT composite.

Keywords: *bioceramics, silicon nitride, hydroxyapatite, grain size, electrospraying*

I. Introduction

Several types of biomaterials have been used for total knee and hip replacements in orthopaedic surgery since the 1970s. Metallic materials, such as titanium alloys and cobalt-chromium have been widely used due to their excellent mechanical strength and corrosion resistance. Nevertheless, the high wear rate and the toxicity of the chemical components imposed the use of non-metallic implant materials like polymers and ceramics [1,2]. Bioinert ceramics, such as alumina (Al_2O_3), zirconia-toughened alumina (ZTA), tetragonal zirconia polycrystals (TZP) or yttria stabilized tetragonal zirconia polycrystals (Y-TZP) have been used for surgical implant devices because of their good physical and mechanical properties (good strength, hardness and wear-resistance) [3,4].

In the case of silicon nitride (Si_3N_4) ceramics, beside its advantageous properties it is possible also to achieve 2- or 3-times better fracture toughness, thanks to its microstructure. The high fracture toughness results from the extended crack path along the surface of the elongated grains [5]. Although there is no chemical reaction between bioinert ceramics (e.g. Si_3N_4) and the living tissue [6], bioactive materials can induce tissue reactions in human body [7]. Hydroxyapatite (HA) is a calcium phosphate ceramic which is widely used for bone reconstruction due to its high bioactivity and biocompatibility [8,9]. Synthesized nanosized hydroxyapatite (nHA) has insufficient mechanical capabilities, consequently it cannot be used in hip replacements as a long-term functional material. However, it is well-known that nHA can be biodegraded by osteoclasts [10]. Usage of a biodegradable and bioactive temporary coating on the implant's surface could induce tissue reactions and help avoid the rejection from the body in the critical early few days, after the operation.

There are numerous deposition techniques which can be used for nHA deposition, including plasma spraying [11], pulsed laser deposition [12] or RF-magnetron sputtering [13]. The aim of this study was to produce nHA coating on silicon nitride (Si_3N_4) implant material with a cost-efficient and well-controllable method, called electrospray deposition (ESD) [14].

To the best of our knowledge, electrosprayed biogenic nanosized hydroxyapatite coatings on Si_3N_4 have not been performed yet. The reason is that due to the low electrical conductivity of the Si_3N_4 substrate, it is hard to form a continuous nHA layer. Nevertheless, multiwall carbon nanotubes addition can drastically change the electric properties of silicon nitride, depending on the carbon addition type and concentration [15]. In or-

*Corresponding authors: tel: +36 1 392 2249,
e-mail: *balazsi.csaba@energia.mta.hu*

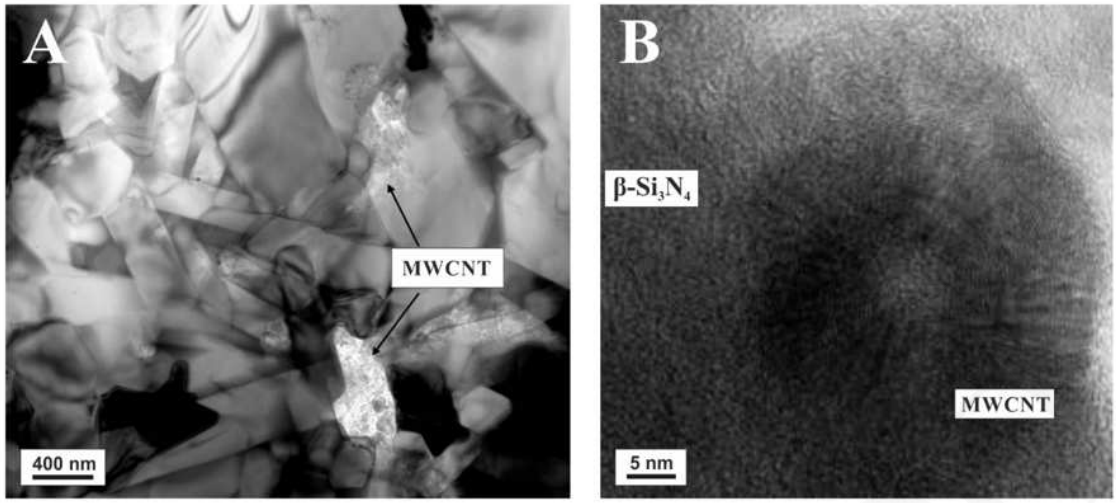

Figure 1. Structural study of Si_3N_4/MWCNT substrate: A) TEM image of sintered composite, B) HREM detail of MWCNT and Si_3N_4 grain boundary

der to increase the electrical conductivity of the substrate, doped Si_3N_4 ceramics with 3 wt.% multiwall carbon nanotubes (MWCNT) have been realized successfully.

II. Materials and methods

2.1. Si_3N_4 and Si_3N_4/MWCNT preparation

The starting powder for silicon nitride preparation consisted of 90 wt.% Si_3N_4 (Ube, SN-ESP), 6 wt.% Y_2O_3 (H.C. Starck, grade C) and 4 wt.% Al_2O_3 (Alcoa, A16). The mixture was milled in a highly efficient attrition mill (Union Process, 01HD-HDDM) in a silicon nitride tank, using ZrO_2 balls (1 mm in diameter) and ethanol at 3000 rpm for 5 h. 10 wt.% polyethylene glycol (PEG) was dissolved in the ethanol and used as a surfactant. In case of Si_3N_4/MWCNT sample preparation we added 3 wt.% MWCNT to the mixture after a 4.5 h milling process, and for the last 30 min we decreased the frequency of rotation to 600 rpm. The batches contained zirconia as contamination from the balls and agitator discs. 5 g zirconia got into the 100 g silicon nitride starting powder from the agitator discs. The quantity of zirconia contamination originating from the balls was roughly the same. The mixtures had been dried and sieved with a filter with mesh size of 100 μm. After the dry pressing at 220 MPa, a 300 °C heat treatment was applied to eliminate the PEG from the samples. Hot isostatic pressing (HIP) was performed at 1700 °C in high purity nitrogen by a two-step sinter-HIP method using boron nitride (BN) embedding powder. The gas pressure was 20 MPa with 3 h holding time. The heating rate did not exceed 25 °C/min [16,17]. The microstructure of Si_3N_4/MWCNT is shown by transmission electron microscopy (TEM) and high-resolution transmission microscopy (HREM) in Fig. 1.

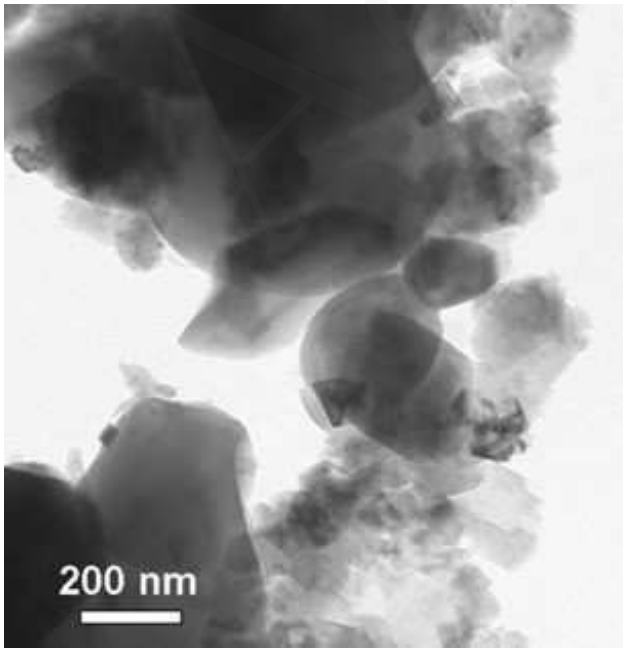

Figure 2. TEM image of nanosized hydroxyapatite powder

2.2. Synthesis of nanosized hydroxyapatite

The synthesis of nHA was based on a previous study with slight modifications [18]. Crushed raw eggshells were calcined at 900 °C for 10 h. The 5-hour milling process of the calcined eggshells was performed in the attrition mill (Union Process, 01HD-HDDM) with phosphoric acid (the same mass quantity as the eggshell powder sample) in ethanol. Zirconia agitators, tank and 1 mm diameter sized ZrO_2 balls at 2500 rpm have been employed. The heat treatment of the milled nanosized powder at 900 °C for 2 h resulted in HA phases, but further milling was necessary (with the same parameters) without phosphoric acid to reach the appropriate 100–200 nm particle size. The microstructure of the nanosized hydroxyapatite is shown by TEM in Fig. 2.

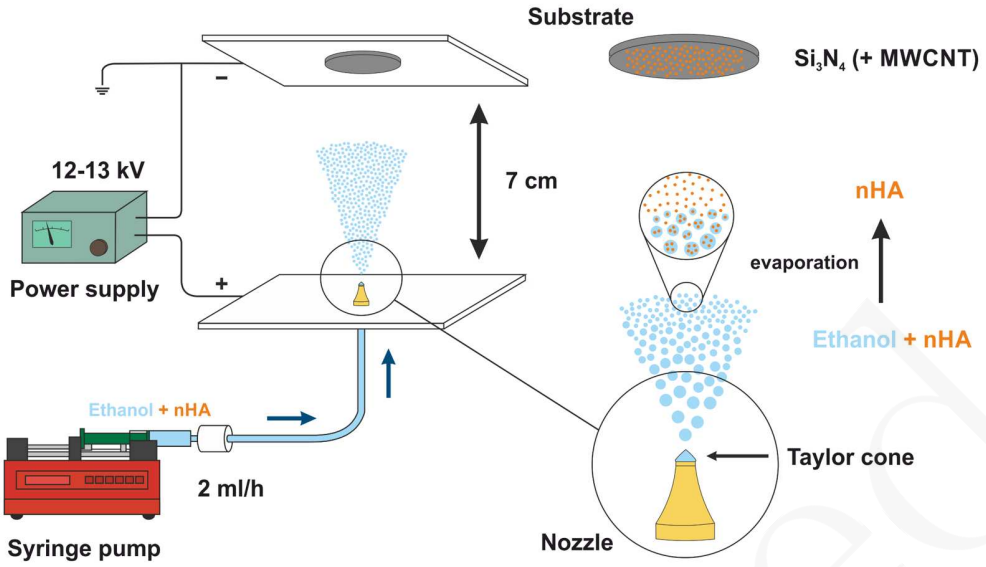

Figure 3. Schematic diagram of the electrospray deposition set-up

2.3. Electrospray deposition (ESD)

In this technique, a syringe was filled with a suspension (e.g. ethanol + nHA crystals). This liquid was pumped through a metal capillary (the nozzle) with a fixed flow rate. An electrode was attached to the nozzle, while another electrode was attached to the substrate (e.g. Si_3N_4/MWCNT composite). A constant potential difference was applied between the nozzle and the grounded substrate. At a specific high voltage, the accumulation of charges on the liquid surface led to the formation of Taylor cone. At higher potential difference, the electrostatic forces overcame the surface tension and droplets left the surface of the cone, accelerated toward the grounded substrate by the electric field. Due to the evaporation of the volatile solvent (ethanol), only the solid particles (nHA) accumulated at the substrate (Fig. 3) [19–21].

In this study, the process was performed at room temperature by an Inovenso Ne100 electrospinning/ electrospraying machine. The suspension (25 ml ethanol, 0.125 g nHA) was stirred by a magnetic stirrer device and shook in ultrasonic bath for 15 minutes respectively. The suspension was forced through a 0.95 mm inside diameter sized copper nozzle with an automated syringe pump at a flow rate of 1 ml/h or 2 ml/h. A voltage of 12–13 kV was applied. The distance between the nozzle and the substrate was 7 cm and a spraying time of 15 and 45 min was used.

2.4. Characterization methods

X-ray diffractometry (XRD, Bruker AXS D8 with Cu Kα radiation) measurements were performed for the phase determination. Transmission electron microscopy (TEM, Philips CM-20 with 200 kV) and high-resolution electron microscopy (HREM, JEOL 3010 with 300 kV) were used for structural investigations of silicon nitride and hydroxyapatite. The morphological properties and the thickness of the deposited layers were studied by a field emission scanning electron microscope (LEO 1540 XB) equipped with Everhart-Thornley and InLens secondary electron detectors. A Röntec Si(Li) detector and Bruker Esprit 1.9 software were used for the EDX measurements. The electrical resistance of the substrates was measured by a Voltcraft VC140 Digital Multimeter.

III. Results and discussion

3.1. Electrospray deposition on Si_3N_4 substrate

In the first experiment pure silicon nitride ceramic was used as a substrate for the nHA deposition. The electrical resistance of the Si_3N_4 (Fig. 4A) was over the 20 MΩ measuring limit, therefore it can be considered as an insulator. The Taylor cone was not stable during the 45-minute-long electrospray deposition process. Small alteration of the applied voltage was necessary between 12 and 13 kV from time to time, in order to avoid the collapse of the cone. The flow rate of the suspension was 2 ml/h. The nHA grains occurred only sparsely on the surface (Fig. 4B), however accumulation was also observable at a few places (Fig. 4C,D). Continuous nHA layer was not formed due to the high electrical resistance of the silicon nitride substrate (Fig. 4). The characteristic phases of the Si_3N_4 substrate were determined by XRD. β-Si_3N_4 and yttrium zirconium oxide ($Zr_{0.72}Y_{0.28}O_{1.862}$) peaks can be noticed on the diffractogram (Fig. 5). $Zr_{0.72}Y_{0.28}O_{1.862}$ was caused by Y_2O_3 and the contamination from zirconia balls and agitator discs. α-Si_3N_4 peaks are missing, consequently it can be stated that complete phase transformation happened from the α-Si_3N_4 powder to β-Si_3N_4 during the hot isostatic pressing. The small amount of nHA on the surface did not cause distinct peaks on the diffractogram. In order to increase the electrical conductivity

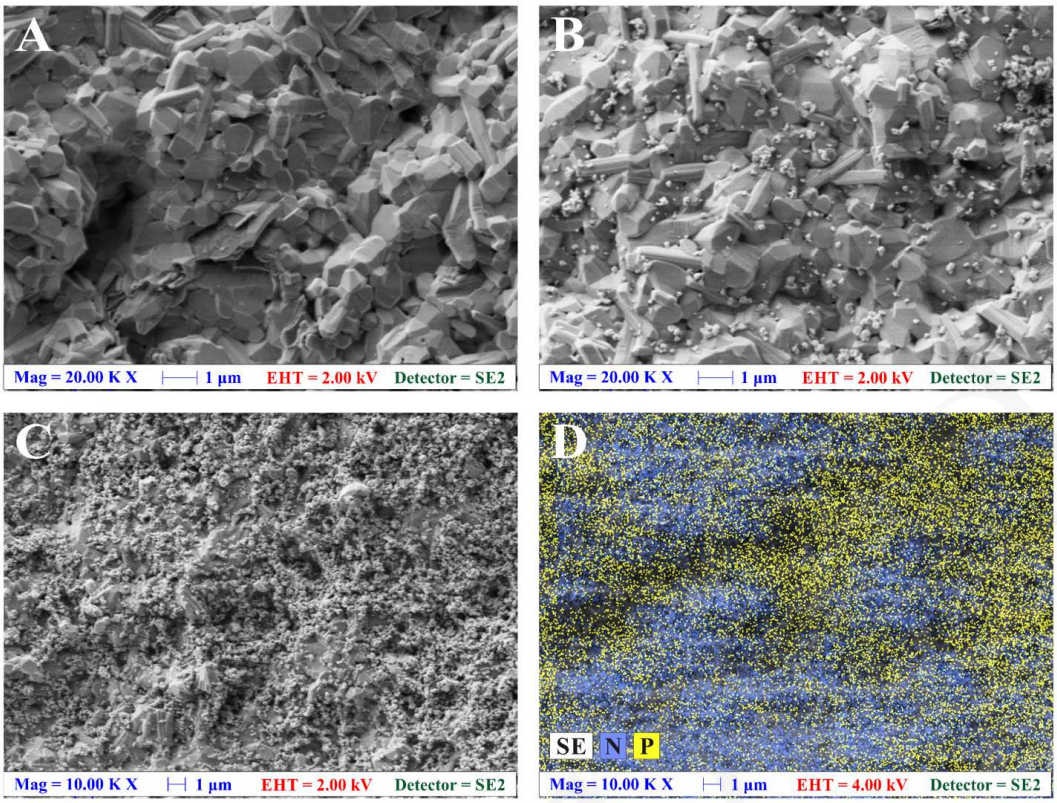

Figure 4. SEM images of the Si_3N_4 substrate before (A) and after (B, C, D) the electrospray deposition process. A) pure Si_3N_4, B) sparsely deposited nHA grains on the Si_3N_4 surface, C) accumulation of nHA crystals, D) X-ray elemental mapping image from the nHA accumulation part

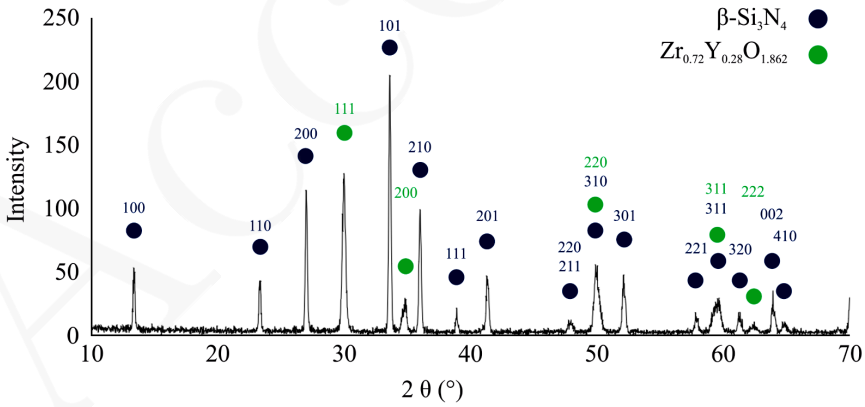

Figure 5. X-ray diffractogram of the Si_3N_4 surface after electrospray deposition

of the substrate and produce thin and continuous nHA coating, we doped the Si_3N_4 ceramics with 3 wt.% multiwall carbon nanotubes (MWCNT).

3.2. Electrospray deposition on Si_3N_4/MWCNT substrate

The surface of Si_3N_4/MWCNT composite was more porous, compared to the pure Si_3N_4 (Fig. 6A). The electrical resistance values of the two Si_3N_4/MWCNT discs were between 5 and 6 kΩ which means that the electrical conductivity of the substrates has been successfully increased with carbon nanotube addition. Usage of the Si_3N_4/MWCNT instead of pure silicon nitride as a substrate, resulted in a stable Taylor cone during the electrospray deposition process. In this case voltage alteration was unnecessary, therefore constant voltage was applied for two samples. 12.8 kV voltage, 1 ml/h flow rate and 15-minute-long spraying time were used for the first experiment. It can be seen both on the secondary electron and X-ray elemental mapping images, that the nHA layer did not cover the Si_3N_4/MWCNT substrate completely (Fig. 6B,C). Nevertheless, the amount of nHA particles on the Si_3N_4/MWCNT composite's surface is much higher after the deposition process than

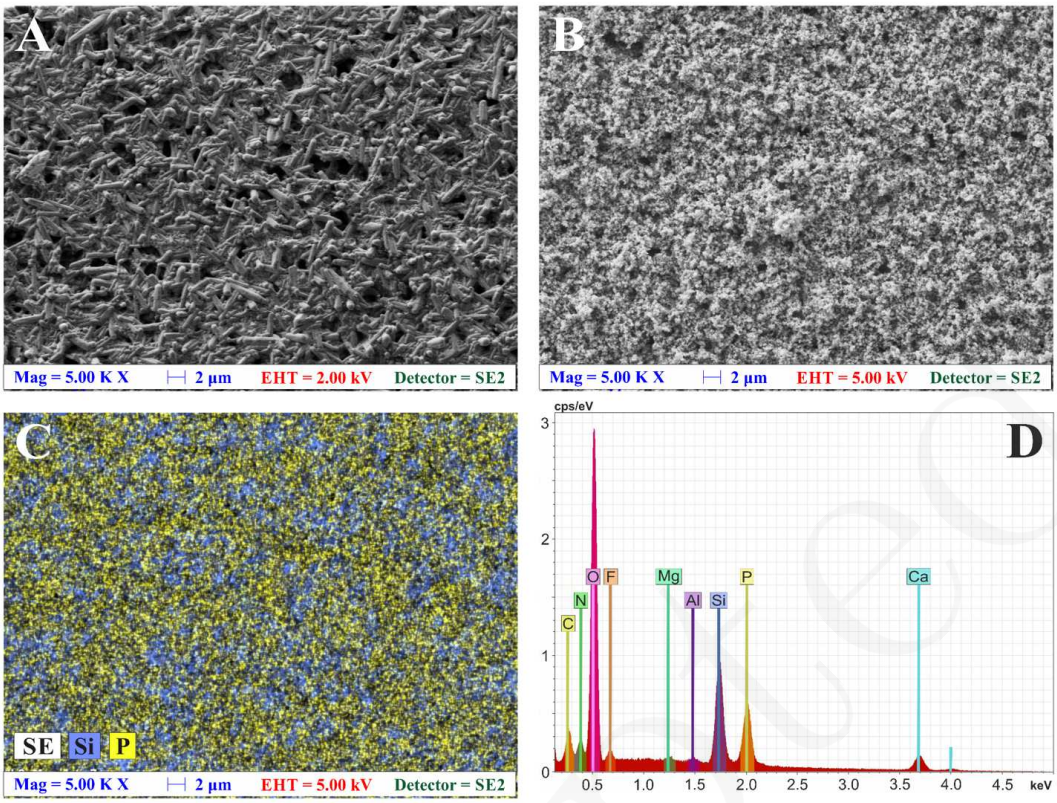

Figure 6. SEM and EDX images of the Si_3N_4/MWCNT substrate before (A) and after (B, C, D) the 15-minute-long electrospray deposition process. A) pure Si_3N_4/MWCNT, B) nHA layer on the Si_3N_4/MWCNT surface, C) X-ray elemental mapping image of the electrosprayed nHA on the Si_3N_4/MWCNT surface, D) EDX spectrum of the electrosprayed nHA coating

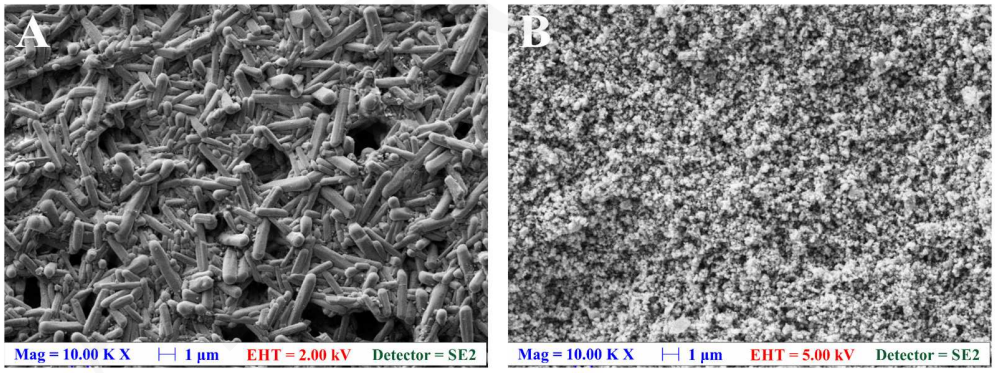

Figure 7. SEM images of the Si_3N_4/MWCNT substrate before (A) and after (B) the 45-minute-long ESD process. A) pure Si_3N_4/MWCNT, B) continuous nHA coating on the Si_3N_4/MWCNT surface

the amount of nHA on the pure Si_3N_4 in the previous experiment. EDX measurement revealed that the synthesized nanosized hydroxyapatite contained Mg and F in the crystal lattice beside Ca, O and P elements (Fig. 6D). The chemical formula of hydroxyapatite is $Ca_5(PO_4)_3OH$, however the apatite lattice is very tolerant to substitutions, vacancies or solid solutions. OH can be replaced by F while Mg and Na can substitute for Ca [22–24]. The source of F could be the Teflon spacers in the attrition mill. Si and N peaks can also be seen, because the produced nHA layer is thin and it does not cover the substrate completely (Fig. 6D).

In order to produce thicker layer, we changed the spraying time from 15 to 45 minutes and the flow rate from 1 ml/h to 2 ml/h (Figs. 7–9). This time, the nHA grains covered the whole substrate. Using a constant 12.8 kV voltage and 45-minute-long spraying time, a thin (~5 µm) and smooth nHA coating was deposited on the MWCNT doped silicon nitride (Si_3N_4) implant material (Figs. 7B and 9B). The phase identification of nanohydroxyapatite coating was possible with XRD, because in contrast to the pure silicon nitride substrate, the amount of nHA crystals was above the detection limit (Fig. 8). Carbon nanotubes were not observable

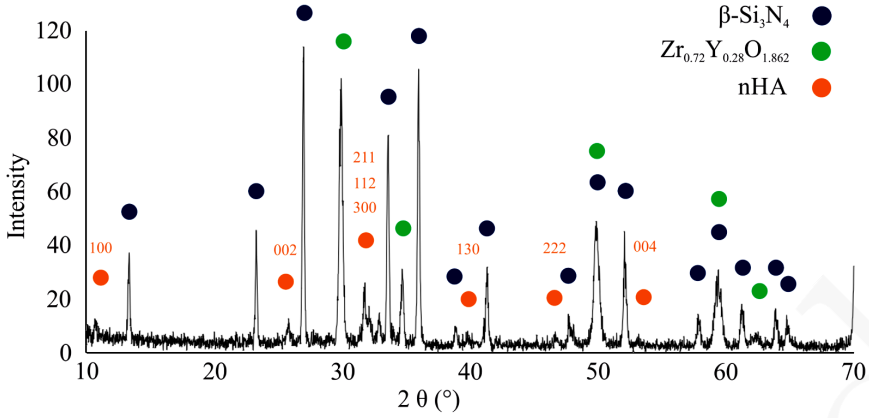

Figure 8. X-ray diffractogram of the Si_3N_4/MWCNT surface after 45-minute-long ESD

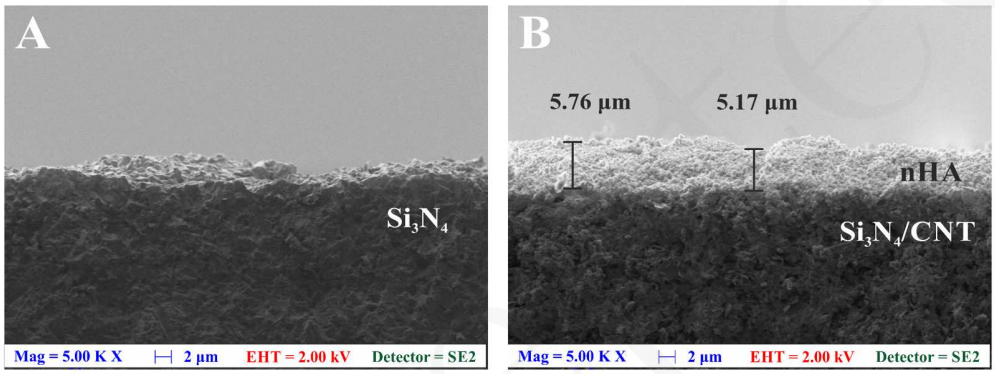

Figure 9. Transverse sections of the Si_3N_4 (A) and Si_3N_4/MWCNT (B) substrates after 45-minute-long ESD process with the same deposition parameters

on the Si_3N_4/MWCNT composite's surface with the scanning electron microscope, and the typical peaks (2θ = 26°) were missing from the XRD diffractogram also. Nevertheless, aggregated MWCNTs were found between the silicon nitride crystals in the transverse section by TEM (Fig. 1), which means the carbon nanotubes occur only inside the Si_3N_4 ceramic.

IV. Conclusions

The aim of this study was to produce thin nHA layer on silicon nitride implant material by electrospray deposition. To the best of our knowledge, this is the first time that electrosprayed nanosized hydroxyapatite coatings were deposited on a ceramics, although this method is more cost-efficient than other widely used deposition techniques like plasma spraying, pulsed laser deposition or RF-magnetron sputtering.

In case of electrospraying, electrically conductive materials are required as substrates. Ceramics are mostly insulators, therefore special treatments (e.g. doping) are necessary for creating appropriate substrates for the deposition process. Multiwall carbon nanotubes (3 wt.%) were ideal dopants for increasing the conductivity of Si_3N_4. The carbon nanotubes occurred only inside the substrate. Using the same deposition parameters, a thin (5 µm) nHA coating was deposited on the MWCNT doped silicon nitride after 45 minutes, while continuous nHA layer could not form on the pure (insulator) Si_3N_4 surface during this time.

Acknowledgement: Special thanks to L. Illés for the SEM /EDX, S. Gurbán for electrical measurements, Dr. Z.E. Horváth for the XRD measurements (MTA EK). Support from the European Union Seventh Framework Programme FP7/2007-2013 under grant agreement "HypOrth" No. 602398, FLAG-ERA "Multifunctional Ceramic/Graphene Coatings for New Emerging Applications" and COST Action CA15102 Solutions for Critical Raw Materials under Extreme Conditions is highly acknowledged.

References

1. C.C. Gomes, L.M. Moreira, V.J.S.V. Santos, A.S. Ramos, J.P. Lyon, C.P. Soares, F.V. Santos, "Assessment of the genetic risks of a metallic alloy used in medical implants", *Genet. Mol. Biol.*, **34** [1] (2011) 116–121.
2. M. Saini, Y. Singh, P. Arora, V. Arora, K. Jain, "Implant biomaterials: A comprehensive review", *World J. Clin. Cases*, **3** [1] (2015) 52–57.
3. S.G. Ghalme, A. Mankar, Y. Bhalerao, "Biomaterials in hip joint replacement", *Int. J. Mater. Sci. Eng.*, **4** [2] (2016)

113–125.
4. M. Rahaman, W. Xiao, "Silicon nitride bioceramics in healthcare", *Int. J. Appl. Ceram. Technol.*, **15** [4] (2018) 861–872.
5. Y.S. Zheng, K.M. Knowles, J.M. Vieira, A.B. Lopes, F.J. Oliveira, "Microstructure, toughness and flexural strength of self-reinforced silicon nitride ceramics doped with yttrium oxide and ytterbium oxide", *J. Microscopy*, **201** [2] (2001) 238–249.
6. B. McEntire, M. Rahaman, G. Pezzotti, "Debunking the myth that ceramics are bioinert: Comparison of alumina versus silicon nitride", *Orthopaedic Proceedings*, **98-B** [7] (2018) 28.
7. J. Park, *Bioceramics: Properties, Characterizations, and Applications*, Springer Science & Business Media, 2009.
8. P. Ducheyne, Q. Qiu, "Bioactive ceramics: the effect of surface reactivity on bone formation and bone cell function", *Biomaterials*, **20** [23-24] (1999) 2287–2303.
9. S.-W. Lee, C. Balázsi, K. Balázsi, D.-H. Seo, H.S. Kim, C.-H. Kim, S.-G. Kim, "Comparative study of hydroxyapatite prepared from seashells and eggshells as a bone graft material", *Tissue Eng. Regenerative Med.*, **11** [2] (2014) 113–120.
10. E. Rumpel, E. Wolf, E. Kauschke, V. Bienengräber, T. Bayerlein, T. Gedrange, P. Proff, "The biodegradation of hydroxyapatite bone graft substitutes in vivo", *Folia Morphol.*, **65** [1] (2006) 43–48.
11. L.L. Xu, J.S. Shi, "Study on plasma-spraying coating bioactive ceramics onto silicon nitride surface as composite endosteal implants", *Biomed. Sci. Instrum.*, **33** (1997) 585–589.
12. P.G. Dinda, J. Shin, J. Mazumder, "Pulsed laser deposition of hydroxyapatite thin films on Ti-6Al-4V: effect of heat treatment on structure and properties", *Acta Biomater.*, **5** [5] (2009) 1821–1830.
13. T. Wan, H. Aoki, J. Hikawa, J.H. Lee, "RF-magnetron sputtering technique for producing hydroxyapatite coating film on various substrates", *Biomed. Mater. Eng.*, **17** [5] (2007) 291–297.
14. E.S. Thian, X. Li, J. Huang, M.J. Edirisinghe, W. Bonfield, S.M. Best, "Electrospray deposition of nanohydroxyapatite coatings: A strategy to mimic bone apatite mineral", *Thin Solid Films*, **519** [7] (2011) 2328–2331.
15. C. Balázsi, B. Fényi, N. Hegman, Z. Kövér, F. Wéber, Z. Vértesy, Z. Kónya, I. Kiricsi, L.P. Biró, P. Arató, "Development of CNT/Si_3N_4 composites with improved mechanical and electrical properties", *Composites Part B: Eng.*, **37** [6] (2006) 418–424.
16. B Fényi, P. Arató, F. Wéber, N Hegman, C. Balázsi, "Electrical examination of silicon nitride – carbon composites", *Mater. Sci. Forum*, **589** (2008) 203–208.
17. P. Hvizdos, J. Dusza, C. Balázsi, "Tribological properties of Si_3N_4-graphene nanocomposites", *J. Eur. Ceram. Soc.*, **33** [12] (2013) 2359–2364.
18. C. Balázsi, F. Wéber, Z. Kövér, E. Horváth, C. Németh, "Preparation of calcium-phosphate bioceramics from natural resources", *J. Eur. Ceram. Soc.*, **27** [2-3] (2007) 1601–1606.
19. A.M. Yousaf, O. Mustapha, D.W. Kim, D.S. Kim, K.S. Kim, S.G. Jin, C.S. Yong, Y.S. Youn, Y.-K. Oh, J.O. Kim, H.-G. Choi, "Novel electrosprayed nanospherules for enhanced aqueous solubility and oral bioavailability of poorly water-soluble fenofibrate", *Int. J. Nanomed.*, **11** (2016) 213–221.
20. N. Radacsi, R. Ambrus, T. Szunyogh, P. Szabó-Révész, A. Stankiewitz, A.v.d. Heijden, J.H.t. Horst, "Electrospray crystallization for nanosized pharmaceuticals with improved properties", *Crystal Growth Design*, **12** [7] (2012) 3514–3520.
21. S.C.G. Leeuwenburgh, M.C. Heine, J.G.C. Wolke, S.E. Pratsinis, J. Schoonman, J.A. Jansen, "Morphology of calcium phosphate coatings for biomedical applications deposited using electrostatic spray deposition", *Thin Solid Films*, **503** [1-2] (2006) 69–78.
22. J.C. Elliott, R.M. Wilson, S.E.P. Dowker, "Apatite structures", *Advances in X-ray Analysis*, **45** (2002) 172–181.
23. J.C. Elliott, "Calcium phosphate biominerals", *Rev. Mineral. Geochem.*, **48** [1] (2002) 427–453.
24. Z. Li, J. D. Pasteris, "Chemistry of bone mineral, based on the hypermineralized rostrum of the beaked whale Mesoplodon densirostris", *Am. Mineralogist*, **99** [4] (2014) 645–653.